



# Embroidered electrochemical sensors on gauze for rapid quantification of wound biomarkers



Xiyuan Liu<sup>a</sup>, Peter B. Lillehoj<sup>a,b,\*</sup>

<sup>a</sup> Department of Mechanical Engineering, Michigan State University, East Lansing, MI, USA

<sup>b</sup> Department of Biomedical Engineering, Michigan State University, East Lansing, MI, USA

## ARTICLE INFO

### Keywords:

Electrochemical sensor  
Gauze  
Embroidery  
Wearable  
Wound monitoring

## ABSTRACT

Electrochemical sensors are an attractive platform for analytical measurements due to their high sensitivity, portability and fast response time. These attributes also make electrochemical sensors well suited for wearable applications which require excellent flexibility and durability. Towards this end, we have developed a robust electrochemical sensor on gauze via a unique embroidery fabrication process for quantitative measurements of wound biomarkers. For proof of principle, this biosensor was used to detect uric acid, a biomarker for wound severity and healing, in simulated wound fluid which exhibits high specificity, good linearity from 0 to 800  $\mu\text{M}$ , and excellent reproducibility. Continuous sensing of uric acid was also performed using this biosensor which reveals that it can generate consistent and accurate measurements for up to 7 h. Experiments to evaluate the robustness of the embroidered gauze sensor demonstrate that it offers excellent resilience against mechanical stress and deformation, making it a promising wearable platform for assessing and monitoring wound status in situ.

## 1. Introduction

Wearable sensors have gained considerable attention in recent years due to their capacity for real-time health and environmental monitoring. In particular, wearable chemical sensors enable analytical measurements of bodily fluids in situ minimizing the time, labor and costs associated with conventional laboratory-based assays. Prior wearable sensors have mainly been applied for assessing overall health via monitoring analytes in bodily fluids, such as sweat (Gao et al., 2016; Kim et al., 2014; Modali et al., 2016), tears (Chu et al., 2011; Yan et al., 2011), and interstitial fluid (Collison et al., 1999; Kool et al., 2007). Another important application where wearable sensors show promise is wound monitoring. Chronic wounds are a rapidly growing public health threat and place a significant burden on the healthcare system and economy. In the United States alone, it is estimated that chronic wounds affect 5.7 million people costing the U.S. healthcare system \$25 billion annually (Frykberg and Banks, 2015; Sen et al., 2009). One of the main challenges associated with wound management is difficulty in accurately assessing wound status, which is largely based on visual inspection of the wound and patient feedback (Chrisman, 2010). Therefore, researchers have been developing wearable sensors to monitor various physiological and biochemical parameters of wounds, such as wound pH (Guinovart et al., 2014; Nocke et al., 2012), bacterial

metabolites (Ciani et al., 2012; Sharp and Davis, 2008; Zhou et al., 2011), temperature (Matzeu et al., 2011; Moser and Gijss, 2007), moisture (McColl et al., 2007, 2009) and endogenous biomarkers (Kassal et al., 2015; Sharp et al., 2008). These devices, as well as most wearable chemical sensors, employ screen-printed electrodes which are simple to fabricate, inexpensive and offer good analytical performance. However, screen printing is poorly suited for loosely woven materials, such as gauze and wound dressing, due to their high porosity and textured surface. Furthermore, screen-printed sensors on gauze are prone to damage resulting from mechanical strain and deformation in response to the wearer's movement, which limits their practicality for *ex vivo* wound sensing.

Here, we demonstrate a gauze-based embroidered sensor for in situ electrochemical measurements of wound biomarkers. This is made possible via a unique embroidery fabrication process which enables the creation of robust, flexible electrodes on loosely woven materials, including gauze and wound dressing. For proof of principle, this biosensor was used for quantitative measurements of uric acid in simulated wound fluid. Uric acid is associated with oxidative stress and bacterial infection within the wound area (Kassal et al., 2015; McLister et al., 2014; Sharp and Davis, 2008) suggesting its usefulness as an indicator for wound infection. Recent studies have also shown that uric acid levels in wound fluid is highly correlated with wound severity and

\* Corresponding author at: Department of Mechanical Engineering, Michigan State University, East Lansing, MI, USA.  
E-mail address: [lillehoj@egr.msu.edu](mailto:lillehoj@egr.msu.edu) (P.B. Lillehoj).

healing, making it a promising biomarker for assessing wound status and monitoring the progress of wound healing (Fernandez et al., 2012, 2013). In addition to single measurements, this biosensor was used for continuous measurements of uric acid for up to 7 h to evaluate its utility for wound monitoring. Lastly, we compared the robustness of our embroidered sensor with a screen-printed sensor, and evaluated the effects of mechanical deformation on its analytical performance.

## 2. Experimental

### 2.1. Biochemicals and reagents

Uric acid, glucose, L-lactate, creatinine, human serum albumin and potassium ferrocyanide ( $K_3[Fe(CN)_6]$ ) were purchased from Sigma-Aldrich (St. Louis, MO). Uricase and Ringer's solution were purchased from Fisher Scientific (Pittsburgh, PA). Silver/silver chloride (Ag/AgCl) and carbon inks were purchased from Conductive Compounds Inc. (Hudson, NH) and Kapton was purchased from McMaster-Carr (Elmhurst, IL). Deionized (DI) water ( $18.3 M\Omega\text{-cm}^{-1}$ ) was generated using a Barnstead Smart2Pure water purification system. PBS powder (pH 7.4) was purchased from Sigma-Aldrich (St. Louis, MO) and prepared as directed using DI water. Simulated wound fluid was prepared as previously described (Pawar et al., 2014) with minor modifications. Briefly, human serum albumin (2% w/w) was added to Ringer's solution and vortexed to generate a uniform fluid consistency. Analytes were serially diluted in simulated wound fluid at room temperature, and samples were freshly prepared prior to measurements.

### 2.2. Thread preparation and characterization

Each electrochemical sensor consists of three electrodes; a reference electrode (RE), working electrode (WE) and counter electrode (CE), which was fabricated using ink-coated thread. Briefly, polyester thread (Brothers International, Bridgewater, NJ) was soaked in carbon or Ag/AgCl ink and cured at 120 °C for 40 min. Carbon-coated thread was used for the WE and CE, and Ag/AgCl-coated thread was used for the RE. Soldering flux (Kester, Itasca, IL) was applied to the Ag/AgCl thread using a flux pen prior to the ink coating process to minimize oxidation of the ink.

### 2.3. Sensor design and fabrication

Sensors were designed using AutoCAD software (Autodesk, Vernon Hills, IL), converted into an embroidery file using SewArt software (S & S Computing), and embroidered onto gauze using a Brothers SE400 computerized embroidery machine. A stabilizer (World Weidner, Ponca City, OK) was used to improve the embroidery quality. Several embroidery parameters, such as the stitch length and stitch density, were optimized to enhance the electrical properties of the electrodes for improved signal consistency and signal-to-noise ratio (SNR). After the electrodes were embroidered, the stabilizer was removed and sensors were cut into individual pieces. Screen-printed sensors were fabricated by screen printing Ag/AgCl and carbon inks onto gauze using a Kapton stencil. The stencil was designed using AutoCAD software and fabricated using a CO<sub>2</sub> laser cutter (Universal Laser Systems, Scottsdale, AZ). After screen-printing, the sensors were heated for 4 min at 120 °C and cut into individual pieces. Uricase solution (10 mg/mL) was drop cast on the WE and dried for at least 1 h prior to measurements. Prepared sensors were used immediately or stored at ambient conditions for up to 3 days prior to experiments.

### 2.4. Sensor characterization

Scanning electron microscopy (SEM) was used to examine the morphology of ink-coated thread and embroidered electrodes. SEM

images were captured using a JOEL 6620 V scanning electron microscope at 10 kV at 30× or 5000× magnification for both the RE and WE. For sensor stretching experiments, one end of the sensor was affixed to a solid surface using a bar clamp while the other side was attached to a M & A Instruments digital force gauge using a plastic spring clamp.

### 2.5. Electrochemical measurements and data analysis

Amperometric measurements were performed using a multichannel electrochemical workstation (GeneFluidics, Inc. Irwindale, CA). For single measurements, 15 μL of sample was dispensed from the backside of the sensor using a pipette, followed by the application of a 350 mV bias potential. Each measurement was performed using a new sensor. For uric acid monitoring, 20 μL of sample was dispensed from the backside of the sensor using a pipette, followed by amperometric detection at 350 mV and the application of 100 μL of Ringer's solution to flush the WE. Measurements were performed at 1 h intervals using the same sensor. All measurements were performed at room temperature under ambient conditions. A one-tailed Student's *t*-test was used for comparison between flat and bent sensors where a *p* value < 0.05 was considered significant.

## 3. Results and discussion

### 3.1. Characterizing embroidered sensors

In this work, we used a computerized embroidery machine which offers high flexibility in regards to sensor design, configuration and placement. In contrast to most wearable textiles, gauze is highly porous and delicate, making it difficult to embroider. Therefore, a stabilizer film was used to enhance the rigidity of the gauze, which improved the embroidery quality. Additionally, we optimized several embroidery parameters, such as the thread tension, stitch angle, stitch length and stitch density, to enhance the quality of the electrodes. To accommodate the stretchability of the gauze, the thread tension was adjusted to the lowest setting, which minimized tangling of the thread and generated uniform and consistent embroidered patterns. The stitch angle is the angle between the stitching and the horizontal axis (Schematic S1 in Supplementary Information) and influences the weave pattern and robustness of the embroidered features. We found that a stitch angle of 30 – 45° improved the embroidery quality by increasing the strain of stitches without deforming the underlying gauze. Stitch length and stitch density were optimized to 0.5 mm and 0.2 mm, respectively, which resulted in good electrode uniformity while minimizing the electrical resistance of the electrodes. Using these optimized parameters, we were able to fabricate electrochemical sensors onto commercial gauze and wound dressing (Fig. 1a). To demonstrate the flexibility of this approach, we fabricated electrochemical sensors with various geometries and configurations (Fig. 1b). For example, multiple sensors can be fabricated for multiplexed detection or electrodes with different sizes can be generated to accommodate commercial or custom electrochemical instrumentation. Additionally, sensors can be customized into unique designs, such as symbols or logos, making them less obtrusive and conspicuous.

SEM images of the WE and RE were obtained to briefly study their surface morphology. From Fig. 2b, d, we can observe that the stitches are tightly-sewn together and firmly integrated into the underlying gauze, which enhances the electrical conductivity and robustness of the biosensor. Furthermore, the interstitial spacing between the stitches provides a high surface area for the liquid sample, thereby enhancing the electrochemical reaction and improving the detection signal. Close-up SEM images of the WE and RE show that the threads are uniformly coated with carbon (Fig. 2c) and Ag/AgCl (Fig. 2e) with good surface coverage, even after undergoing the embroidery process.

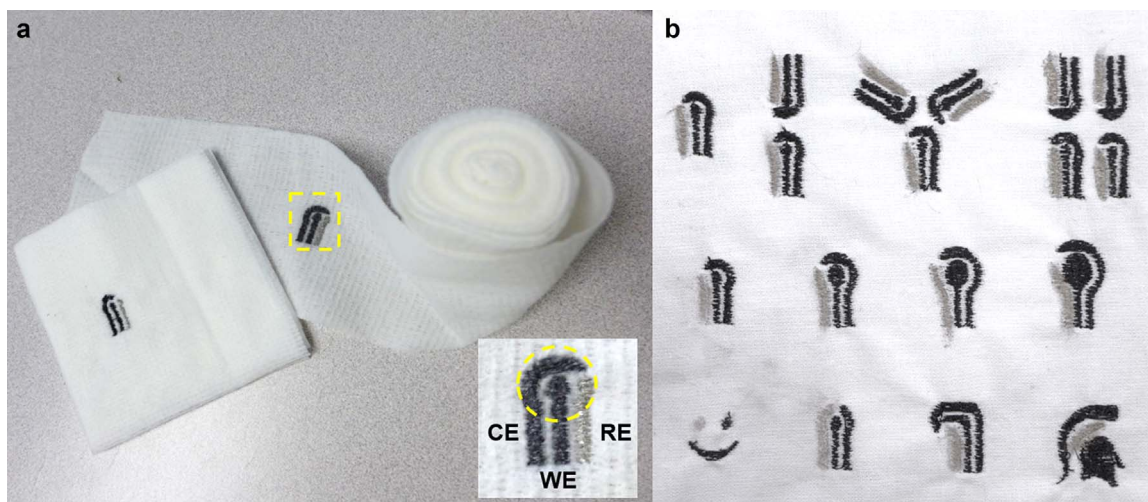


**Fig. 1.** (a) Embroidered electrochemical sensors on gauze and wound dressing. Inset shows a close-up image of the sensor. The dashed circle represents the sensing region. (b) Customized electrochemical sensors and sensor arrays fabricated via embroidery.

### 3.2. Analytical performance of embroidered sensors

To evaluate the effectiveness of our embroidered gauze sensor for analytical sensing, we used it for quantitative measurements of uric acid in simulated wound fluid. Samples were dispensed on the backside of the gauze to simulate wound fluid leakage and were quickly absorbed by the biosensors due to the high wettability of the thread and gauze. Amperometric measurements were performed after 1 min, which was sufficient time for the sample to be fully absorbed and generate a stable electrochemical reaction. Chronoamperometric signals at each concentration of uric acid were clearly distinguishable from the baseline and from each other (Fig. 3a). The signal during the final 10 s of each chronoamperogram was averaged and taken as the final value, and used to generate a calibration plot (Fig. 3b). A direct correlation between the uric acid concentration and generated electrochemical current was observed (correlation coefficient,  $R^2$  of 0.995) over the tested concentration range (0 – 800  $\mu\text{M}$ ), which encompasses the levels in chronic wound fluids (Tregrove et al., 1996). In addition, each data point exhibits small SDs of < 7% over three individual measurements obtained using new sensors, which demonstrates the high reproducibility of this biosensor.

We also tested the selectivity of the uric acid assay by performing measurements of samples containing other analytes. For these experi-

ments, we used simulated wound fluid spiked with glucose, lactate, creatinine and uric acid at concentrations of 2 mM, 10 mM, 120  $\mu\text{M}$  and 400  $\mu\text{M}$ , respectively, which are similar to physiological levels found in wound fluid (Tregrove et al., 1996). As shown in Fig. 3c, only the uric acid sample generated a substantial signal ( $\text{SNR} \sim 7$ ), while the irrelevant targets generated negligible signals similar to that of the non-spiked sample, which was used as a blank control. These results suggest that our embroidered gauze sensor is capable of highly specific measurements in complex biofluid samples with a low likelihood of interference caused by nonspecific analytes.

### 3.3. Uric acid monitoring

To evaluate the utility of our gauze biosensor for wound monitoring, we performed continuous measurements of uric acid over the course of 7 h using the same sensor. Uric acid in simulated wound fluid (600  $\mu\text{M}$ ) was applied to the sensor every hour followed by amperometric detection. Typically in wound care practice, gauze is used in conjunction with a primary dressing to provide adequate wound coverage and fluid drainage. To mimic this scenario, the biosensor was wrapped around a gauze pad and covered with an additional layer of gauze. After each measurement, 100  $\mu\text{L}$  of Ringer's solution was applied to the biosensor

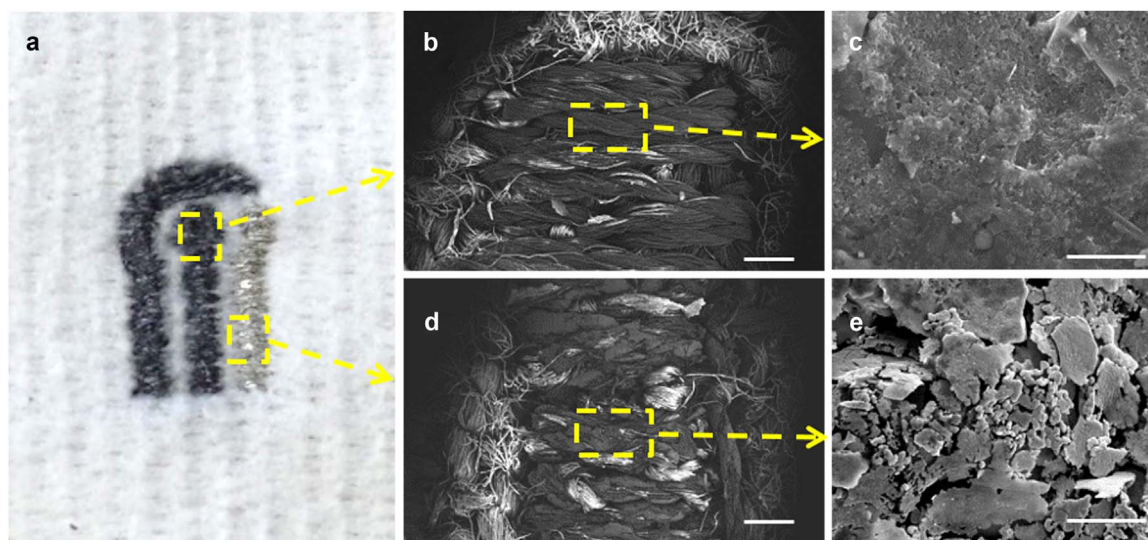


**Fig. 2.** (a) Embroidered electrochemical sensor on gauze. SEM images of the WE (b) and RE (c) at 30 $\times$  magnification. Scale bar, 500  $\mu\text{m}$ . Close-up SEM images of carbon-coated thread (d) and Ag/AgCl-coated thread (e) at 5000 $\times$  magnification. Scale bar, 5  $\mu\text{m}$ .

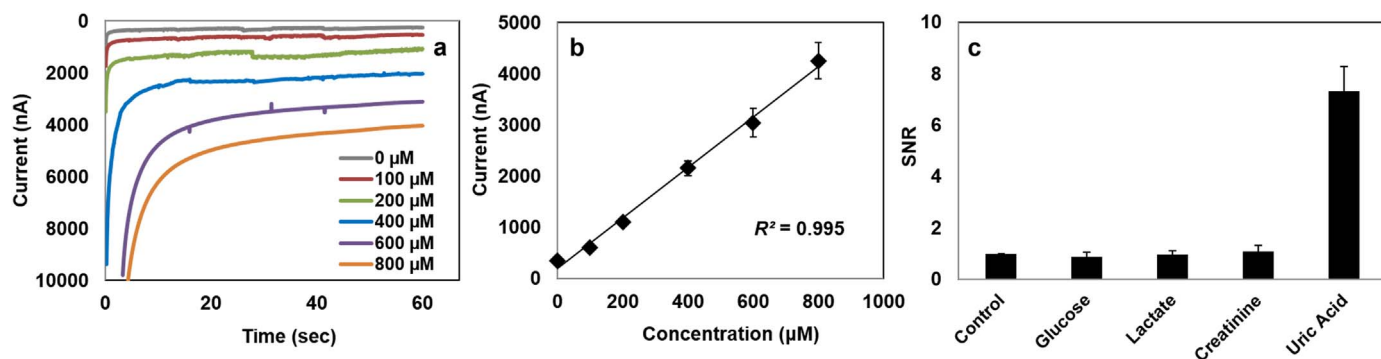


**Fig. 3.** (a) Chronoamperograms of simulated wound fluid spiked with uric acid at concentrations of 0  $\mu\text{M}$ , 100  $\mu\text{M}$ , 200  $\mu\text{M}$ , 400  $\mu\text{M}$ , 600  $\mu\text{M}$  and 800  $\mu\text{M}$ . (b) Calibration plot of generated current vs. uric acid concentration. Each data point represents mean  $\pm$  SD of three measurements of the amperometric signal averaged over the final 10 s of the chronoamperograms. (c) Specificity of the uric acid assay using simulated wound fluid samples containing glucose (2 mM), lactate (10 mM), creatinine (120  $\mu\text{M}$ ) and uric acid (400  $\mu\text{M}$ ), and non-spiked simulated wound fluid (control). Each bar represents the mean  $\pm$  SD of three separate measurements obtained using new sensors.

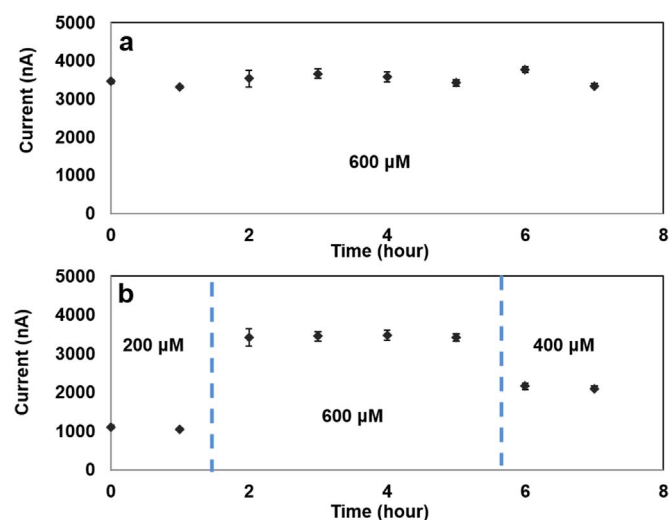


**Fig. 4.** Uric acid monitoring over the course of 7 h using simulated wound fluid containing 600  $\mu\text{M}$  (a), and varying concentrations (b) of uric acid. Each data point represents the mean  $\pm$  SD of three separate measurements using three new sensors.

to flush the sensing region. This process should not interfere with the wound healing process or present any problems for the patient since Ringer's solution is a suitable liquid for wound irrigation (Cutting and Westgate, 2012). As shown in Fig. 4a, the detection signals were consistent throughout the 7 h experiment exhibiting a small coefficient of variance (COV) of 0.05. These results indicate that our embroidered biosensor can generate consistent measurements for several hours without experiencing any loss of performance due to biofouling.

We also tested the performance of our biosensor in response to dynamic changes in the analyte concentration to more accurately mimic the wound healing process. Specifically, it has been shown that uric acid levels in wound fluid significantly decrease later in the wound healing processing due to catabolism by microbial uricase (Sharp and Davis, 2008). To mimic this scenario, we performed multiple measurements of samples containing different concentrations of uric acid over the course of 7 h using the same sensor. Samples containing 200  $\mu\text{M}$  were initially dispensed, followed by samples containing 600  $\mu\text{M}$  at hours 2, 3, 4, 5 and 400  $\mu\text{M}$  at hours 6 and 7. As shown in Fig. 4b, the sensor accurately responded to the dynamic changes of uric acid concentration in the samples. Furthermore, the detection signals are consistent with those generated from single measurements (Fig. 3b), even after being exposed to multiple samples with varying concentrations. These results indicate that our gauze biosensor offers excellent accuracy and repeatability, making it suitable for wound monitoring, particularly wounds that require frequent ( $> 2\times$  per day) dressing

changings (Sood et al., 2013). For applications requiring less frequent dressing changings, the electrodes can be modified with a biocompatible coating, such as chitosan, permitting for a longer operation period (Bulwan et al., 2012).

### 3.4. Sensor durability testing

An important consideration for wearable sensors is the influence of mechanical deformation on the analytical performance. To evaluate the mechanical durability of our embroidered gauze sensor, we manually folded and flattened the biosensors for up to 100 cycles (Fig. 5a, b) and performed measurements of uric acid (200  $\mu\text{M}$ ) in simulated wound fluid at intervals of 5, 10, 25, 50 and 100 bending cycles. Measurements were also performed at the same intervals using sensors that did not undergo folding. By comparing the detection signals from folded and unfolded sensors (Fig. 5c), we found no significant difference ( $p > 0.292$ ) in the analytical performance due to mechanical deformation for up to 100 bending cycles. To mimic the mechanical stress on the biosensor due to the wearer's movement, we evaluated the analytical performance in response to deformation occurring simultaneously while the measurement was carried out. Amperometric measurements of uric acid in simulated wound fluid were performed using sensors that were positioned flat (Fig. 5d) and bent at 90° (Fig. 5e, f) while the signal was being recorded. As shown in Fig. 5g, there is no significant difference ( $p > 0.181$ ) in the detection performance between the two sets of sensors from 0 to 800  $\mu\text{M}$ . Furthermore, the signals generated from the bent sensors maintained a highly linear response ( $R^2 = 0.994$ ) similar to those of the flat sensors with low SDs across multiple measurements using new sensors. This collective data shows that mechanical deformation has a minimal impact on the performance of our embroidered gauze sensor, suggesting that it will be able to maintain high accuracy and reproducibility under instances of repeated deformation for wearable sensing applications.

We also evaluated the mechanical resilience of our embroidered gauze sensor and compared it with a screen-printed sensor by subjecting both sensors to mechanical stretching as shown in Fig. 6. While sensors can be screen-printed on gauze (Fig. 6a), the electrodes begin to crack after a stretching force of 2.6 N (Fig. 6b). In contrast, there was no observable damage to the embroidered sensor at the same stretching force. Upon further stretching, the embroidered electrodes remained intact with no damage even as the gauze began to tear (Fig. 6c). Cyclic voltammetry was used to investigate the electrochemical performance of both sensors in response to mechanical stretching. Prior to stretching, the cyclic voltammogram of the screen-printed sensor shows good electroactivity and similar performance (i.e. reversibility, anodic peak currents) as the embroidered sensor. However, the screen-printed sensor exhibits significant loss of functionality after stretching generating a nearly zero response signal (Fig. 6c). In contrast, the cyclic

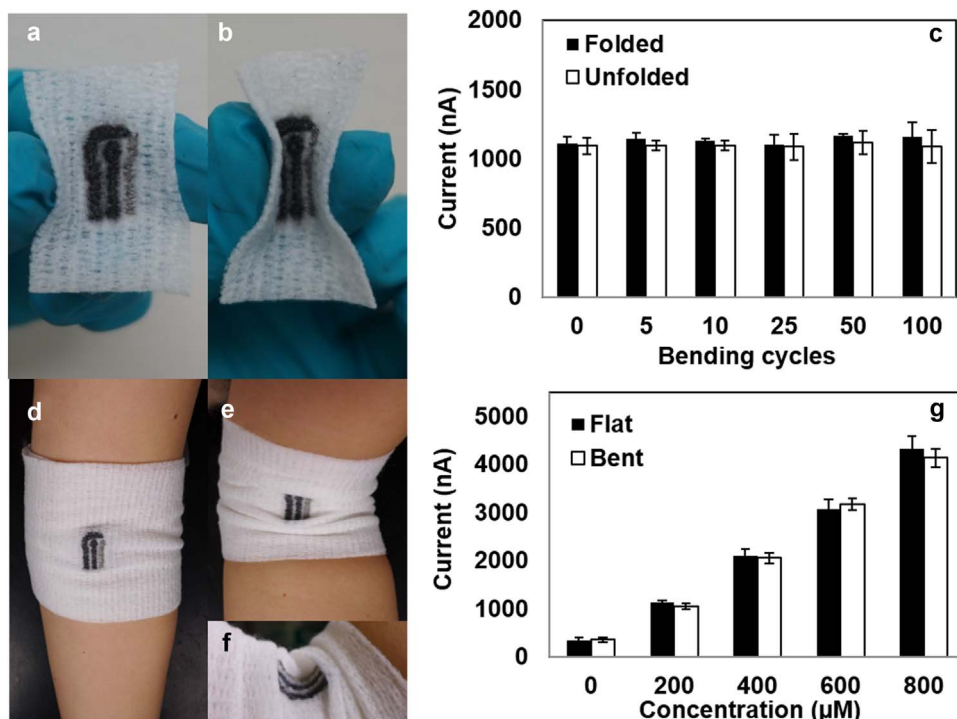


**Fig. 5.** Bend testing of the embroidered gauze biosensor. Images of the sensor before (a) and after (b) folding. (c) Amperometric measurements of uric acid (200 μM) in simulated wound fluid using folded and unfolded sensors. Images of the sensor positioned flat (d) and bent at 90° (e, f), while wrapped around an arm. (g) Amperometric measurements of uric acid in simulated wound fluid using flat or bent sensors. Each bar represents the mean ± SD of three separate measurements using new sensors.

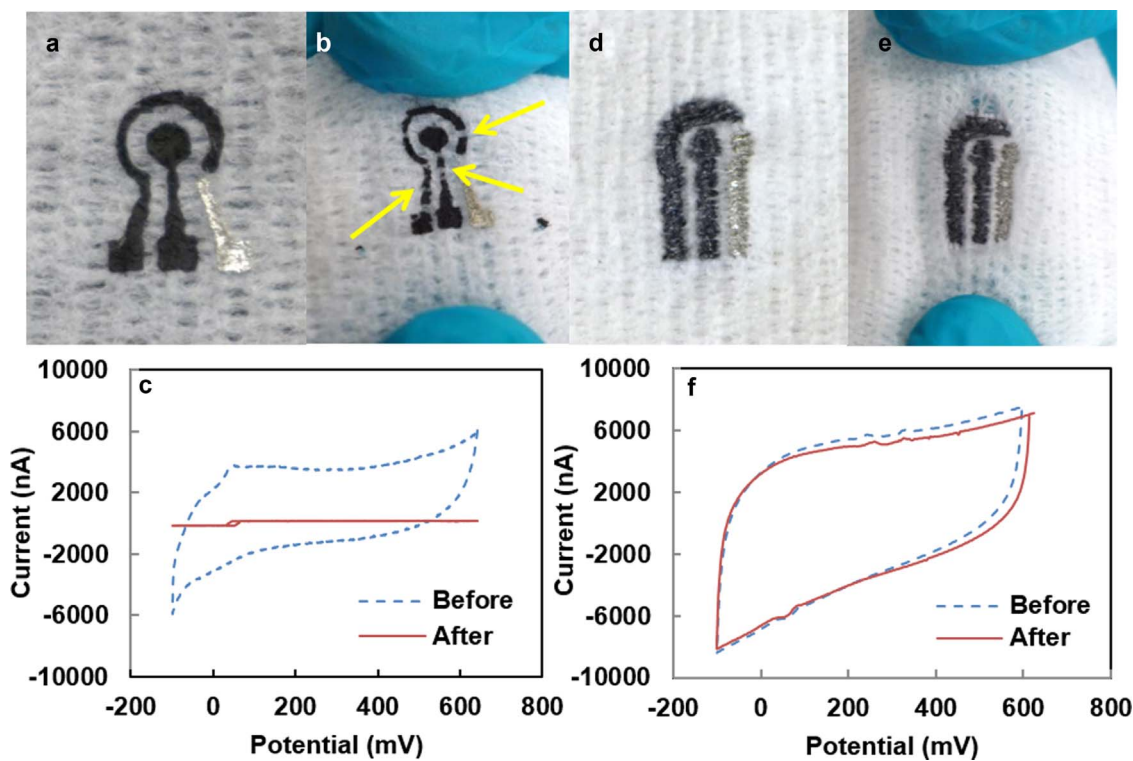


**Fig. 6.** Comparison of screen-printed and embroidered gauze biosensors in response to mechanical stretching. Images of a screen-printed sensor before (a) and after (b) stretching, and corresponding cyclic voltammetry measurements (c). Arrows indicate electrode cracking due to stretching. Images of an embroidered biosensor before (d) and after (e) stretching, and corresponding cyclic voltammetry measurements (f).

voltammograms of the embroidered gauze sensor before and after stretching are nearly identical indicating that it exhibits excellent resilience against mechanical stretching (Fig. 6f).

#### 4. Conclusions

We have presented a robust, flexible electrochemical sensor on gauze fabricated via a unique embroidery process for rapid quantitative measurements of uric acid. This approach offers high flexibility and customization in regards to sensor design and configuration, and is readily amenable to existing manufacturing processes (i.e. embroidery) using off-the-shelf materials. Single and continuous measurements of uric acid in a simulated wound fluid solution demonstrates that this biosensor offers excellent analytical performance for both quantitative wound assessment and monitoring. Experiments to evaluate the robustness of our embroidered biosensor showed its ability to generate consistent and accurate results in response to repeated folding/bending before and during measurements, and exhibit excellent resilience against mechanical strain and deformation. These collective features make our embroidered gauze biosensor a promising technology for wound monitoring applications requiring rapid, accurate measurements on a disposable platform.

#### Acknowledgements

This work was supported by the National Science Foundation CAREER award [grant number ECCS-135056].

#### Appendix A. Supporting information

Supplementary data associated with this article can be found in the online version at doi:10.1016/j.bios.2017.06.053.

#### References

Bulwan, M., Wójcik, K., Zapotoczny, S., Nowakowska, M., 2012. *J. Biomater. Sci. Polym. Ed.* 23, 1963–1980.

- Chrisman, C.A., 2010. *Int. Wound J.* 7, 214–235.
- Chu, M., Shirai, T., Takahashi, D., Arakawa, T., Kudo, H., Sano, K., Sawada, S., Yano, K., Iwasaki, Y., Akiyoshi, K., Mochizuki, M., Mitsubayashi, K., 2011. *Biomed. Microdevices* 13, 603–611.
- Ciani, I., Schulze, H., Corrigan, D.K., Henihan, G., Giraud, G., Terry, J.G., Walton, A.J., Pethig, R., Ghazal, P., Crain, J., Campbell, C.J., Bachmann, T.T., Mount, A.R., 2012. *Biosens. Bioelectron.* 31, 413–418.
- Collision, M.E., Stout, P.J., Glushko, T.S., Pokela, K.N., Mullins-Hirte, D.J., Racchini, J.R., Walter, M.A., Mecca, S.P., Rundquist, J., Allen, J.J., Hilgers, M.E., Hoegh, T.B., 1999. *Clin. Chem.* 45, 1665–1673.
- Cutting, K.F., Westgate, S.J., 2012. *Wounds UK* 8, 130–133.
- Fernandez, M.L., Upton, Z., Edwards, H., Finlayson, K., Shooter, G.K., 2012. *Int. Wound J.* 9, 139–149.
- Fernandez, M.L., Upton, Z., Shooter, G.K., 2013. *Curr. Rheumatol. Rep.* 16, 1–7.
- Frykberg, R.G., Banks, J., 2015. *Adv. Wound Care* 4, 560–582.
- Gao, W., Emaminejad, S., Nyein, H.Y.Y., Challa, S., Chen, K., Peck, A., Fahad, H.M., Ota, H., Shiraki, H., Kiriya, D., Lien, D.-H., Brooks, G.A., Davis, R.W., Javey, A., 2016. *Nature* 529, 509–514.
- Guinovart, T., Valdés-Ramírez, G., Windmiller, J.R., Andrade, F.J., Wang, J., 2014. *Electroanalysis* 26, 1345–1353.
- Kassal, P., Kim, J., Kumar, R., de Araujo, W.R., Steinberg, I.M., Steinberg, M.D., Wang, J., 2015. *Electrochem. Commun.* 56, 6–10.
- Kim, J., Valdés-Ramírez, G., Bandodkar, A.J., Jia, W., Martinez, A.G., Ramírez, J., Mercier, P., Wang, J., 2014. *Analyst* 139, 1632–1636.
- Kool, J., Reubsaet, L., Wesseldijk, F., Maravilha, R.T., Pinkse, M.W., D'Santos, C.S., van Hilten, J.J., Zijlstra, F.J., Heck, A.J.R., 2007. *PROTEOMICS* 7, 3638–3650.
- Matzeu, G., Losacco, M., Parducci, E., Pucci, A., Dini, V., Romanelli, M., Francesco, F.D., 2011. *IECON 2011*, (3533–3535).
- McColl, D., Cartlidge, B., Connolly, P., 2007. *Int. J. Surg.* 5, 316–322.
- McColl, D., MacDougall, M., Watret, L., Connolly, P., 2009. *Wounds UK* 5, 94–99.
- McLister, A., Phair, J., Cundell, J., Davis, J., 2014. *Electrochem. Commun.* 40, 96–99.
- Modali, A., Vanjari, S.R.K., Dendukuri, D., 2016. *Electroanalysis* 28, 1276–1282.
- Moser, Y., Gijss, M.A.M., 2007. *J. Microelectromech. Syst.* 16, 1349–1354.
- Nocke, A., Schröter, A., Cherif, C., Gerlach, G., 2012. *Autex Res. J.* 12, 20–22.
- Pawar, H.V., Boateng, J.S., Ayensu, I., Tetteh, J., 2014. *J. Pharm. Sci.* 103, 1720–1733.
- Sen, C.K., Gordillo, G.M., Roy, S., Kirsner, R., Lambert, L., Hunt, T.K., Gottrup, F., Gurtner, G.C., Longaker, M.T., 2009. *Wound Repair Regen.* 17, 763–771.
- Sharp, D., Davis, J., 2008. *Electrochem. Commun.* 10, 709–713.
- Sharp, D., Forsythe, S., Davis, J., 2008. *J. Biochem.* 144, 87–93.
- Sood, A., Granick, M.S., Tomaselli, N.L., 2013. *Adv. Wound Care* 3, 511–529.
- Trengove, N.J., Langton, S.R., Stacey, M.C., 1996. *Wound Repair Regen.* 4, 234–239.
- Yan, Q., Peng, B., Su, G., Cohan, B.E., Major, T.C., Meyerhoff, M.E., 2011. *Anal. Chem.* 83, 8341–8346.
- Zhou, L., Glennon, J.D., Luong, J.H.T., Reen, F.J., O'Gara, F., McSweeney, C., McGlacken, G.P., 2011. *Chem. Commun.* 47, 10347–10349.